IHSS 16: FUNCTIONS OF NATURAL ORGANIC MATTER IN CHANGING ENVIRONMENT

Nature-inspired soluble iron-rich humic compounds: new look at the structure and properties

**Tatiana A. Sorkina · Alexander Yu. Polyakov ·
Natalia A. Kulikova · Anastasia E. Goldt ·
Olga I. Philippova · Alina A. Aseeva ·
Alexey A. Veligzhanin · Yan V. Zubavichus ·
Denis A. Pankratov · Eugene A. Goodilin ·
Irina V. Perminova**

Abstract

Purpose Humic substances (HS) being natural polyelectrolyte macromolecules with complex and disordered molecular structures are a key component of the terrestrial ecosystem. They have remarkable influence on environmental behavior of iron, the essential nutrient for plants. They might be considered as environmental friendly iron deficiency correctors free of synthetic iron (III) chelates disadvantages. The main goal of this study was to obtain water-soluble iron-rich humic compounds (IRHCs) and to evaluate their efficiency as chlorosis correctors.

Materials and methods A facile preparation technique of IRHCs based on low-cost and available parent material was developed. The iron-containing precursor (ferrous sulfate) was added dropwisely into alkaline potassium humate solution under vigorous stirring and pH-control. A detailed characterization both of organic and inorganic parts of the compounds was provided, the iron species identification was carried out jointly by EXAFS and Mössbauer spectroscopy. Bioassay experiments were performed using cucumber *Cucumis sativus* L. as target plants. Plants were grown in modified Hoagland nutrient solution, prepared on deionized water and containing iron in the form of IRHCs. Total iron content in dry plants measured by spectrophotometry after oxidative digestion and the chlorophyll *a* content determined after acetone extraction from fresh plant were used as parameters illustrating plants functional status under iron deficiency condition.

Results and discussion The high solubility (up to 130 g/l) and iron content (about 11 wt%) of the IRHCs obtained allow considering them to be perspective for practical applications. A set of analytical methods has shown that the main iron species in IRHCs are finely dispersed iron (III) oxide and hydroxide nanoparticles. An application of the precursor solution acidification allows to obtain compounds containing a significant part of total iron (up to 30 %) in the form of partly disordered iron (II–III) hydroxysulphate green rust $GR(SO_4^{2-})$. Bioavailability of iron from IRHCs was demonstrated using bioassay in cucumber plants grown up on hydroponics under iron deficiency conditions.

Conclusions The application of iron oxides chemistry for humic substance containing solution was proved to be an effective approach to synthesis of IRHCs. Using bioassay on cucumber plants *C. sativus* L. under iron deficiency conditions, the efficiency of compounds obtained as chlorosis correctors was demonstrated. Application of water-soluble

T. A. Sorkina (✉) · A. A. Aseeva · D. A. Pankratov ·
E. A. Goodilin · I. V. Perminova
Department of Chemistry, Lomonosov Moscow State University,
Moscow, Russia
e-mail: sorkina@org.chem.msu.ru

A. Y. Polyakov · A. E. Goldt · E. A. Goodilin
Department of Materials Science, Lomonosov Moscow State
University, Moscow, Russia

N. A. Kulikova · O. I. Philippova
Department of Soil Science, Lomonosov Moscow State
University, Moscow, Russia

A. A. Veligzhanin · Y. V. Zubavichus
RRC "Kurchatov Institute", Moscow, Russia

IRHCs led to significant increase of chlorophyll a content (up to 415 % of the blank) and iron content in plants (up to 364 % of the blank) grown up on hydroponics.

1 Introduction

Humic substances, the major constituent of soil organic matter, are natural polyelectrolyte macromolecules with disordered molecular structures, including condensed aromatic rings substituted by carboxylic, phenolic, and methoxyl groups and aliphatic fragments. They are a key component of the terrestrial ecosystem, being responsible for many complex chemical reactions in soil (Stevenson 1982) and providing availability of biogenic metals for plants and microorganisms (Aguirre et al. 2009; Chen et al. 2004). Especially remarkable is the influence of HS on environmental behavior of iron (Lobartini et al. 1998; Lovley et al. 1998). Iron, the fourth most widespread element in the Earth's crust and in soils, is essential nutrient for plants. This metal plays a significant role in many processes like chlorophyll and DNA synthesis, reduction of molecular nitrogen and the energy-yielding electron transfer reactions of respiration and photosynthesis (Bell and Dell 2008). Despite of the fact that total iron content of soils vastly exceeds plant's demand (Shenker and Chen 2005), the deficiency of this element is the most common nutritional plant disease. The reason of iron deficiency, manifested as leaf chlorosis, is low availability of iron (III) oxides, forming in soils, especially in calcareous ones (Bitcover and Sieling 1951). The most effective treatment of lime-induced chlorosis is application of synthetic iron (III) chelates such as Fe–DTPA, Fe–EDDHA, etc. (Álvarez-Fernández et al. 2005). The main advantages of these chelates are their stability in alkaline calcareous soil and extreme bioavailability of iron (Anderson 1983). The main disadvantages are a high price, which limits their practical application (Yehuda et al. 2003), and potential negative impact on environment. The primary risk is accumulation of these complexes in soils and agricultural products as well as increasing of heavy metal mobility occurring because of ligands action on contaminated contiguous water ecosystem (Antonopoulou et al. 2007). Moreover, the chelates production requires hazardous reactants, while the ligand photo-degradation leads to formation of toxic products (Chassapis et al. 2010). The environmental friendly solution of the issues mentioned above is application of iron deficiency correctors based on humic substances. The capacity of natural organic matter including HS to alleviate the iron intake

by plants was shown by (Bar-ness and Chen 1991). This ability is connected both with biological activity of organic matter and availability of its endogenous iron. However, the iron content in natural HS commonly does not exceed 1 wt%, and its practical application as chlorosis correctors is economically irrational. The solution is natural HS enriched with bioavailable iron. According to practical requirements, these preparations have to be soluble in water and possess high iron content that does not match the salt or complex, in which amount of iron is limited by quantity of HS acidic groups. Different experimental approaches to obtaining of humic-based iron compounds are described in Chassapis et al. (2010) Horneer et al. (1934), Levinskij (2002), Herjsted (1991), Perez-Sanz et al. (2006), but the chemical forms of iron in these compounds is under discussion. According to Schwertmann and Cornell (2000), in soils with low organic matter content, iron (III) oxides as hematite and goethite dominate, whereas increasing the amount of organic matter lead to goethite when Fe supply is low and to ferrihydrite when Fe supply is higher. At a very high content of organic matter, all iron cations are presented in the form of coordination compounds with organic ligands, rather than in the form of iron oxides. Thus, the most perspective form of metal for iron enriched humic-based material is poor-crystalline iron oxides.

The main goal of this work was to obtain soluble in water iron-rich humic compounds (IRHCs) and to evaluate their efficiency as chlorosis correctors.

2 Materials and methods

2.1 Synthesis of the IRHCs

Water-soluble IRHCs were synthesized according to a modified technique based on the approach published elsewhere (Perminova 2005) using commercially available potassium humate "Sakhalinskiy" (Biomir-2000, Russian Federation). To remove insoluble admixtures, 6 % aqueous solution of the potassium humate was centrifuged (4,000 rpm, 5 min) and the supernatant decanted was dried in vacuum oven VD53 (Binder, Germany). All other reactants were of an analytical grade. All the solutions were prepared using high-purity deionized water.

The potassium humate purified (K–HS) was taken as a parent humic material whereas saturated $FeSO_4$ solution was used as an iron-containing precursor. In order to study the effect of ferrous ions hydrolysis and oxidation in the precursor solution before the reaction, two types of IRHCs were obtained: the first one (Fe–HS-H_2SO_4) was synthesized using $FeSO_4$ saturated solution acidified down to pH 0 using sulfuric acid whereas the second one was obtained without any $FeSO_4$ solution pre-treatment. For the IRHCs

synthesis, the iron-containing precursor was gradually added to the reaction mixture containing 5 % solution of K–HS under vigorous stirring. The syntheses were carried out at room temperature. The pH value of the reaction mixture was maintained at 10.0±0.2 using 1 M KOH during the addition of ferrous sulfate and 1 h after. The products obtained were dried in the vacuum oven.

2.2 Characterization of the IRHCs

The solubility of IRHCs was determined according to the following procedure. The excessive amount of sample was dissolved in deionized water; the mixture was vigorously stirred during 30 min and then centrifuged for 5 min at 7,000 rpm. The 20 ml aliquot of supernatant was taken and dried in vacuum oven. The solubility of IRHCs was calculated from mass of dry powder obtained.

Total iron content in dry samples was determined after oxidative digestion of IRHCs organic part. To digest the organic material, 30 mg of the sample were placed in titanium autoclave. After that, 300 mg of $K_2S_2O_8$ and 1 ml of concentrated HNO_3 were added. The autoclave was heated at 200 °C for 3 h. The digestion products were diluted by deionized water and iron content in the solution obtained was analyzed using o-phenanthroline method on the spectrophotometer Cary 50 (Varian, USA).

Elemental CHN composition of IRHCs was characterized using elemental micro-analyzer Vario Micro cube (Elementar, Germany). Infrared (IR) transmission spectra were recorded using FT IR 200 spectrometer. X-ray powder diffraction (XRD) data for all the samples were collected in a step scan mode at room temperature using Rigaku D/Max 2500 diffractometer with a rotating anode (Cu-Kα radiation, θ–2θ Bragg–Brentano geometry, 25–70° 2θ-range, 0.02° step). Morphology of the samples obtained was characterized using transmission electron microscope (TEM) Leo912 AB Omega (Zeiss, Germany) with accelerating voltage 120 kV.

EXAFS spectra at Fe K-edge were obtained at the Structural Materials Science end-station at the Kurchatov Centre for Synchrotron Radiation and Nanotechnology (Chernyshov et al. 2009). For EXAFS data treatment, the software package IFEFFIT 1.2.11 was used (Newville 2001). Iron (III) synthetic chelate Fe–EDDHA (Aglukon, Germany) and iron (III) trisalicylate obtained in this study according to Mahesh et al. (1979) were used as reference samples for iron local environment investigation. Mössbauer absorption spectra were recorded using a MS1104-EM express Mössbauer spectrometer (MosTek, Russian Federation) with ^{57}Co in a rhodium matrix as the radiation source, activity 3.5 and 10 mCi (Cyclotron, Russian Federation), at temperatures 5, 78, and 298 K. Chemical shifts were measured using α-Fe as a standard. Temperature was maintained within ±3 K.

The spectra were fitted using the least-squares minimization procedure by Univem-MS software (MosTec., Russian Federation) version 9.08.

2.3 Bioassay

Bioassay experiments were carried out using cucumber *Cucumis sativus* L. cv. "Dalnevostochny" as target plants which were grown in modified Hoagland nutrient solution (Kovacs et al. 2005), prepared on deionized water. Iron was introduced in the form of studied samples with metal concentration of 25 μM. Cucumber seeds were germinated in Petri dishes in deionized water at 25 °C for 48 and 24 h in 0.5 mM $CaSO_4$ solution before transferring to nutrient solution. The seedlings were grown in climate chamber with 12 h photoperiod at 25 °C during 7 days. To evaluate the efficiency of IRHCs as correctors of iron chlorosis, such parameters as chlorophylls a content in fresh plants and iron content in the dry ones were used. The content of iron was measured using o-phenantroline method after oxidative digestion of dried plants using digestor DS-8 (Foss Tecator, Italy). The chlorophyll a content was determined after acetone extraction from fresh plant biomass on spectrophotometer Cary 50 (Varian, USA) according to Mokronosov (1994).

3 Results and discussion

3.1 Synthesis and general characteristics of IRHCs

The main idea of the present work was to synthesize soluble in water IRHCs with iron content considerably higher than the one causing insoluble product formation in syntheses of salts or iron-humic chelates. According to Perez-Sanz et al. (2006) the iron content in soluble Fe–HS compounds is limited with quantity of carboxylic group content (CGC), typical values of which are 3.2–4.8 mmol/g for HS (Ritchie and Perdue 2003). Pursuant to (Levinskij 2002) the threshold iron content is estimated as 0.3×CGC that is 6–9 wt% of total iron in dry samples. To achieve higher iron content without solubility loss, a designing of nature-inspired composite structures containing finely dispersed iron species, such as oxides and oxyhydroxides, stabilized by HS was suggested. Since HS stabilize iron oxide species via interaction of acidic groups with the oxide surface, the syntheses of IRHCs were carried out at pH 9–10 for achievement of total deprotonation and activation of carboxylic and phenolic groups. The higher pH can lead to dissolution of iron species in form of hydroxyanions and excessive increase of alkali content in the final product. Moreover the chosen pH range well corresponds both with the ones of intensive iron oxyhydroxides formation and the synthesis conditions

recommended for soluble iron-containing humic compounds elsewhere (Perminova 2005).

Elemental composition of IRHCs characterized with high ash content equal to 68 ± 2 wt%, C 17.8 ± 0.3, H 1.8 ± 0.1, N 0.7 ± 0.1 wt%, and total iron content 11.3 ± 0.4 wt% significantly differed from the composition of initial potassium humate: ash 33.7 wt%, C 31.7, H 3.3, N 1.1 wt% with total iron content 1.0 wt%. The solubility of IRHCs in water at room temperature was rather high (120–130 g/L) and sufficient for practical application. The same applies to iron content (~11 wt%) of IRHCs, which exceeds typical content values of commercially available iron chelates (6–7 wt%).

To get a deeper insight into the metal–ligand bond formation, IR transmission spectroscopy was used. The IR spectra of the IRHCs as well as of initial potassium humate are presented in the Electronic supplementary material (ESM 1). The spectrum of initial humate is typical for sodium and potassium salts of humic acids and contains two strong absorption bands centered at ca. 1,580 and 1,375 cm^{-1} corresponding to νCOO^- (as.) and νCOO^- (sym.) vibrations of deprotonated carboxylic groups, respectively (Stevenson and Goh 1971). Neither shifts of these absorption bands after the synthesis of IRHCs nor additional bands indicating metal-carboxylate complexes formation were detected. At the same time two strong absorption bands centered at ca. 630 and 1,120 cm^{-1} relating to sulfate ion (Nakamoto 1986) appeared in Fe–HS and Fe–HS–H_2SO_4 spectra. The presence of potassium sulfate in IRHCs was also confirmed with XRD results. Weak and very broad features with the positions similar to the strongest reflexes of several iron oxides were found on the XRD patterns too, but could not be resolved and identified. Thus, XRD analysis suggested us that synthesized IRHCs contain finely dispersed and practically X-ray amorphous iron oxides.

It was also found that ca. 60 % of each powder could be separated by a magnet from potassium sulfate crystals slightly covered by HS. Such an empirically determined magnetic behavior can also be caused by the presence of magnetically ordered iron oxide phases in IRHCs. Some amount of Fe–HS–H_2SO_4 sample was separated by strong NdFeB magnet and magnetic part was studied by TEM in order to visualize finely dispersed iron oxide phases.

3.2 Iron species identification

According to electron micrographs, Fe–HS–H_2SO_4 sample contains a lot of tiny plate-like and rod-like nanoparticles with the sizes from 2 to 20 nm (Fig 1a, b). Selected area electron diffraction (SAED) pattern (see Fig. 1c) has two uniform rings indicating the presence of finely dispersed polycrystalline species. The positions of the rings coincide with the brightest ones of finely dispersed feroxyhyte,

magnetite, and maghemite; however, accurate identification of the particles phase composition is not possible. The particles which lead to appearance of the second diffraction ring are highlighted on the dark field image (see Fig. 1d). The other scattered and isolated reflexes in SAED pattern (see Fig. 1c) were attributed to well-crystalline admixtures, first of all to potassium sulfate, originated either from initial potassium humate or formed as by-products in the synthesis of IRHC. The presence of iron in the region used for SAED were clearly shown by EEL spectrum on Fe–$L_{2,3}$ edge (see Fig. 1e) .
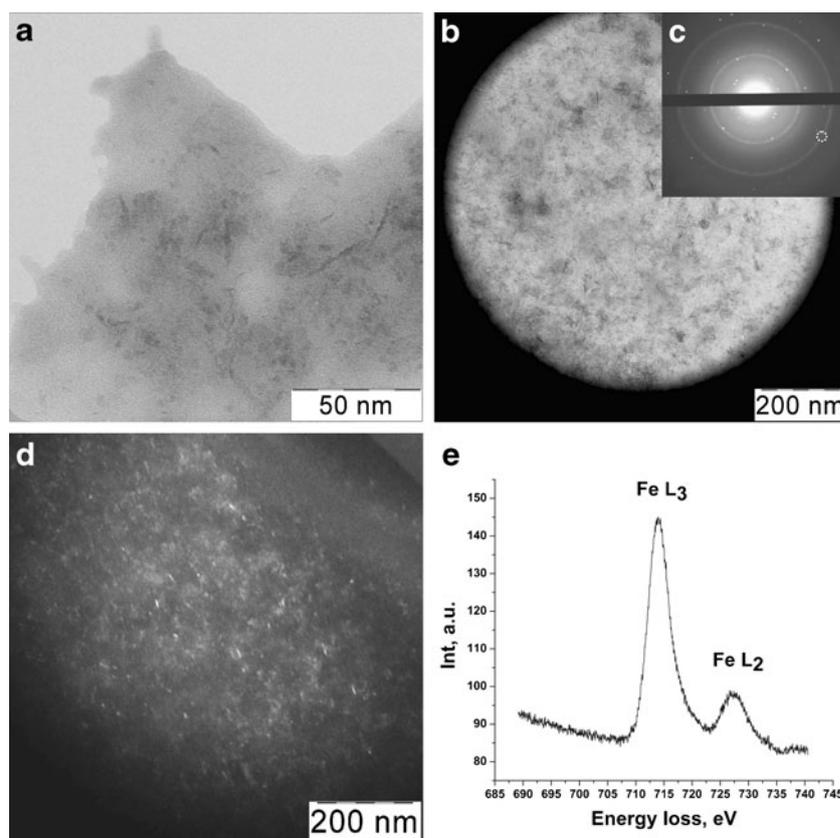
An averaged iron local environment in the samples was studied by EXAFS spectroscopy at Fe K-edge. Several iron-containing compounds were used as reference standards. Typical Fe–EDDHA fertilizer with iron surrounded by four oxygen and two nitrogen atoms (Bell and Dell 2008) and Fe(Sal)$_3$ containing iron surrounded by six oxygen atoms (Mahesh et al. 1979) were used as a references with different octahedral iron environment. Feroxyhyte nanoparticles in situ stabilized by HS (δ'-FeOOH/HS) (Polyakov et al. 2012) were used as a sample with high content of humic-entrapped finely dispersed iron oxyhydroxide possessing iron environment describing as linked {Fe(O,OH)$_6$} octahedra, whereas bulk α-Fe$_2$O$_3$ was used as well-crystalline sample with typical oxide environment of iron linked {FeO$_6$} octahedra.

EXAFS spectra were recorded and Fourier-transformed in the region of k from 2 to 13 Å^{-1} and presented on Fig. 2. The k-space EXAFS data are presented in ESM 2. The k region is quite narrow resulting in the presence of a number of minor peaks and shoulders in the magnitude of Fourier-transformation. Nevertheless, all the samples studied have distantly resembling spectrum shapes in the first coordination sphere (FCS) region corresponding to octahedrally-coordinated iron. However, Fe–EDDHA spectrum has pronounced difference in the FCS region due to the presence of two nitrogen atoms in coordination octahedron.

Significant resemblance of the FCS signals in Fe–HS and Fe–HS–H_2SO_4 spectra with that of Fe(Sal)$_3$ and iron oxides indicates octahedral {FeO$_6$} environment in IRHCs. The parameters of iron local environment in Fe(Sal)$_3$, IRHCs, δ'-FeOOH/HS and α-Fe$_2$O$_3$ calculated using one sphere approximation of EXAFS spectra are listed in the Table 1. The distance to neighboring oxygen atoms and Debye–Waller factors were fitted to achieve agreement with experimental spectra. In order to obtain coordination numbers of Fe sites in the samples overall amplitude multiplier was fixed at the value of 0.8 for all the samples.

Slightly decreased coordination numbers of iron in IRHCs (see Table 1) was attributed to distortion of {FeO$_6$} coordination octahedra. The signal from the second coordination sphere well-resolved for bulk α-Fe$_2$O$_3$ sample vanishes in δ'-FeOOH/HS and IRHCs spectra and completely

Fig. 1 TEM micrographs, SAED and EELS data for magnetic part of Fe–HS-H$_2$SO$_4$ sample: **a** representative TEM image of finely dispersed nanoparticles found; **b** selected area of the sample and **c** electron diffraction (SAED) registered from it (the outlined part of the second diffraction ring was used for dark field image formation); **d** dark field image with highlighted nanoparticles which form the second diffraction ring in SAED; **e** EEL spectrum on Fe-L$_{2,3}$ edge registered from the sample region used for SAED

disappears in the case of Fe(Sal)$_3$. Therefore, we can suggest that finely dispersed iron oxides or oxyhydroxides with distorted octahedral {FeO$_6$} FCS and partly disordered second coordination sphere are the main types of iron species in IRHCs obtained.

Since identification of phase composition of finely dispersed iron species in the IRHCs was found to be a difficult issue, Mössbauer spectroscopic study providing important

Fig. 2 Fourier-transformed EXAFS spectra of IRHCs and reference standards selected. Gray rectangle indicates the window in *r*-space used for parameters calculation by one sphere approximation. *Asterisk*, the synthesis and physicochemical characterization of δ′-FeOOH/HS sample are reported in (Polyakov et al. 2012)

information about chemical and magnetic environment of ^{57}Fe probe atoms was carried out.

The Mössbauer spectra of all analyzed samples registered at room temperature could be fitted with the set of doublets. The isomer shifts (δ) and quadrupole splittings (Δ) of iron in the samples studied are graphically presented in Fig. 3.

The most part of iron (III) hyperfine parameters in the samples are in the range (δ from 0.35 to 0.39, Δ from 0.57 to 1.05 mm/s), that is in good agreement with data published for iron-humic compounds (Dickson et al. 1980; Hansen and Mosbaek 1970; Lakatos et al. 1977). However, the ones of trisalicylate (δ 0.48, Δ1.75 and δ 0.41, Δ1.60 mm/s) significantly differ from the rest. These parameters illustrate that iron (III) local environment in this chelate does not match to the one in IRHCs. Moreover, the Mössbauer parameters analysis has shown that Fe–HS–H$_2$SO$_4$ sample contained iron (II) species with parameters (δ 1.12, Δ 2.38 mm/s). To get more information about iron species in IRHCs and their interactions with HS Mössbauer, spectra at 78 and 5 K were taken (Fig. 4).
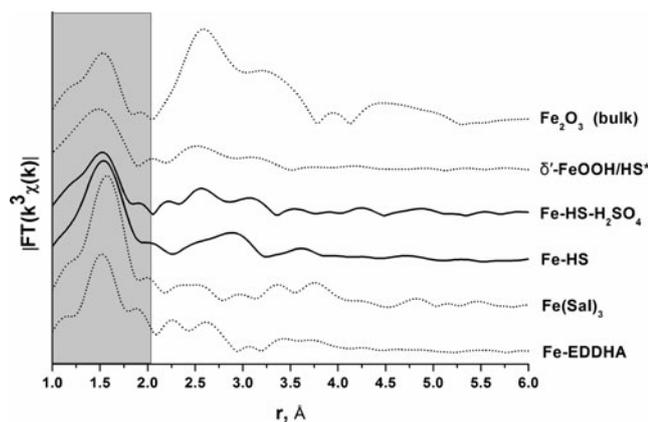
Temperature-dependent Mössbauer spectra show that paramagnetic signals of iron(II) become more pronounced with lowering the temperature from 298 to 78 K (see Fig. 4), that is typical for amorphous compounds, while the same parameter of iron (III) does not change significantly, that, in turn, is typically for crystalline substances. The spectrum at 5 K was fitted with two doublets and two sextets. The

Table 1 The parameters of the first coordination sphere of Fe in IRHCs and reference standards with {FeO$_6$} iron environment calculated using one sphere approximation of EXAFS spectra (R_f, reliability factor; R_{Fe-O}, the distance between Fe and O atoms in the first coordination sphere; σ^2_O, Debye–Waller factor for O atom)

Sample	R_f, %	R_{Fe-O}, Å	Coordination number	σ^2_O, Å^2
Fe(Sal)$_3$	1.53	1.964 (9)	6.0±0.6	0.009 (1)
Fe–HS	0.27	1.964 (5)	5.0±0.3	0.009 (6)
Fe–HS-H$_2$SO$_4$	1.44	1.961 (4)	5.3±0.2	0.011 (5)
δ'-FeOOH/HS	1.99	1.96 (2)	6.0±0.1	0.011 (3)
α-Fe$_2$O$_3$	4.00	1.97 (1)	6.0±0.0	0.011 (1)

transition of some part of iron (III) atoms to the magnetically ordered state occurs between 78 and 5 K. This fact finally confirms that the iron (III) exists in the form of finely dispersed ferric oxide compounds. The final identification was carried out by analysis of hyperfine parameters obtained at 5 K (Table 2).

According to the hyperfine parameters given in Cornell and Schwertmann (2003) the sextets C1 and C2 (Table 3) may be related to lepidocrocite γ-FeOOH, feroxyhyte δ'-FeOOH, or maghemite γ-Fe$_2$O$_3$. More precise identification of the iron (III) oxide or hydroxide phases is difficult because published data usually correspond to bulk compounds but not to finely dispersed nanoparticles. The doublets C3 and C4 were ascribed to iron(II–III) hydroxysulphate green rust GR(SO$_4^{2-}$) (Refait et al. 2003). The stabilization of iron (II) in the form of GR(SO$_4^{2-}$) explains the increasing of its paramagnetic signals at cooling caused by weakening of thermal vibration in partly disordered GR phase.

Thus, the results of the different analytical techniques demonstrate that the main iron species in IRHCs are finely
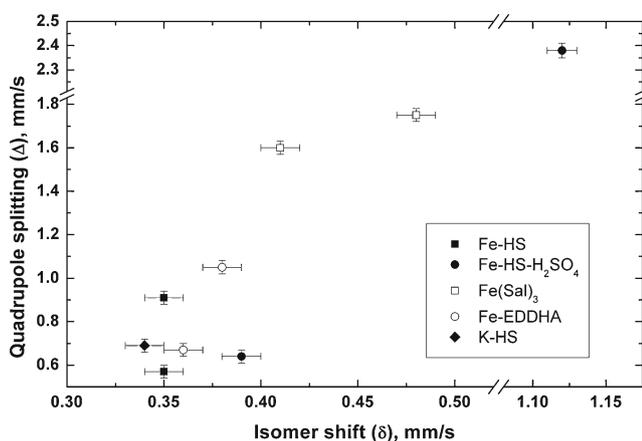
dispersed ferric oxide and hydroxide nanoparticles, moreover the presence of green rust GR(SO$_4^{2-}$) stabilized in the humic "matrix" were ascertained in Fe–HS–H$_2$SO$_4$ sample prepared using acidified iron-containing precursor. Such a role of the acidification of the initial FeSO$_4$ solution can be related to the significant supression of the rate of spontaneous Fe^{2+} oxidation by dissolved O$_2$ at pH 0–3 (Morgan and Lahav 2007). Moreover, it is well-known that in aqueous medium at pH 0 dissolved iron exists in the form of Fe^{2+} and Fe^{3+} ions which are non-hydrolyzed (Cornell and Schwertmann 2003), thus the acidification of FeSO$_4$ solution protects ferrous ions from both premature oxidation and hydrolysis. The acidified precursor was added gradually into alkaline potassium humate solution under vigorous stirring and pH-control. However, humic acids precipitate from solutions because of its insolubility at pH<1. Thus, the droplets of the FeSO$_4$ solution with pH 0 added into the reaction mixture containing potassium humate may cause local coagulation of humic macromolecules which leads to formation of thick but dense microshells. So long as HS possesses considerable reducing activity, these microshells not only slow down the iron oxide and oxyhydroxide crystals growth but also promote the iron (II) species stabilization. Thus this study proves that the targeted synthesis of IRHCs with different iron species and content can be developed using traditional principles of iron oxides chemistry as it was previously shown for feroxyhyte nanoparticles in (Polyakov et al. 2012).
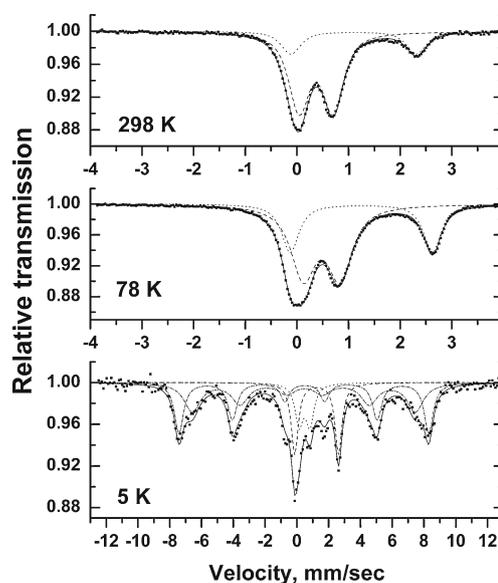
Fig. 4 Mössbauer spectra of Fe–HS–H$_2$SO$_4$ at 298, 78 and 5 K (*straight lines*—the summary fits, *dashed line*—iron (II) doublet, *dotted line*—iron (III) doublet, *chain lines*—sextets of magnetically ordered phases). The transition of some iron (III) atoms to magnetically ordered state occurring between 78 and 5 K illustrates that the sample contains finely dispersed magnetic nanoparticles

Fig. 3 Isomer shifts (δ, millimeter per second) related to α-Fe and quadrupole splittings (Δ, millimeter per second) obtained from Mossbauer spectra registered at 298 K of IRHCs and reference samples

Table 2 Mössbauer hyperfine parameters of the sample Fe–HS-H$_2$SO$_4$ ($\delta \pm 0.01$ mm s^{-1}, isomer shift relative to α-Fe; $\Delta \pm$ 0.01 mm s^{-1} quadrupole splitting or shift; Γ_{exp}, the full line width at half height; $H_{in} \pm$ 0.1 kOe, internal magnetic field (kOe))

T, K	Component	δ mm/s	Δ	Γ_{exp}	H_{in} kOe	Area fraction, %
298	A1	1.12	2.38	0.49	–	30
	A2	0.39	0.64	0.51	–	70
78	B1	1.25	2.75	0.41	–	33
	B2	0.48	0.71	0.58	–	67
5	C1	1.25	2.76	0.53	–	18
	C2	0.47	−0.06	0.67	488.1	35
	C3	0.46	−0.05	1.23	436.1	35
	C4	0.48	0.68	0.60	–	12

3.3 Bioassay

To evaluate the bioavailability of iron in compounds obtained and their efficiency as iron deficiency correctors the bioassay experiments on hydroponics were carried out. The cucumber *C. sativus* L. was selected as target plant because it is very sensitive to iron deficiency and is usually tested in similar experiments (Kovacs et al. 2005; Yehuda et al. 2003). Among all parameters characterizing the functioning of the plant, chlorophyll *a* and iron content were selected as the most informative ones in the case of iron deficiency. The chlorophyll *a* is responsible for energy transformation (Walsh et al. 1995) and total iron content characterizes the iron availability. Table 3 presents bioassay results.

Application of IRHCs led both to a significant increase in chlorophyll *a* and iron content in plants (see Table 3). The iron content in blank experiments was of 67 μg g^{-1} that is typical for iron deficient plants (Shenker and Chen 2005) and increased up to 120–243 μg g^{-1} in the presence of studied IRHCs. According to iron content, following descending order was observed: Fe–EDDHA>Fe–HS-H$_2$SO$_4$>Fe–HS>K–HS, while initial iron concentration in nutrient solutions was equal to 25 μM for all the cases. That finding was consistent with the generally accepted assumption on higher bioavailability of chelated iron and Fe(II) as

compared to Fe(III) for plants with strategy I (Romheld and Merschner 1986). Therefore, the greater iron content in plants treated with Fe–HS-H$_2$SO$_4$ in comparison with Fe–HS might be explained by a significant Fe(II) fraction (up to 30 %) in Fe–HS-H$_2$SO$_4$ sample. Notwithstanding the highest iron availability in case of Fe–EDDHA, the treatment of the plants with that preparation did not lead to the greatest chlorophyll *a* content. The sequence of chlorophyll *a* amounts was as follows: Fe–HS-H$_2$SO$_4$>Fe–EDDHA≈Fe–HS>K–HS, that was indicative of the role of humic moiety of IRHCs in the chlorophyll synthesis. This might be also due to a synergetic effect of bioavailable iron and HS possessing their own biological activity and stimulating properties (Muscolo et al. 2007).

4 Conclusions

The application of iron oxides chemistry for humic substance containing solution was proved to be an effective approach of synthesis of IRHCs. A facile technique for synthesis of IRHCs with high solubility in water (up to 130 g/l) and high iron content (about 11 wt%) based on low-cost and available parent material was developed. Using a set of analytical methods, it was shown that the main iron species in IRHCs are finely dispersed iron (III) oxide and hydroxide nanoparticles. Acidification of the precursor solution allows to obtain compounds, containing significant part of total iron (up to 30 %) in the form of partly disordered iron (II–III) hydroxysulphate green rust GR(SO$_4$$^{2-}$). Using bioassay on cucumber plants under iron deficiency condition, the availability of iron in obtained compounds and its efficiency as chlorosis correctors is demonstrated.

Table 3 Chlorophyll *a* content in fresh cucumber leaves and total iron content in dried plants treated with IRCHs, Fe–EDDHA and K–HS

	Chlorophyll *a* content		Total Fe content	
	mg g^{-1} [a]	% blank	μg g^{-1} [a]	% blank
Blank	0.38±0.03	100	67±10	100
Fe–EDDHA	1.40±0.19	369	504±30	755
Fe–HS	1.36±0.16	358	180±32	269
Fe–HS–H$_2$SO$_4$	1.58±0.06	415	243±31	364
K–HS	1.25±0.01	329	120±28	180

[a] Standard deviation, n=15

References

Aguirre E, Lemenager D, Bacaicoa E, Fuentes M, Baigorri R, Zamarreno AM, Garcıa-Mina JM (2009) The root application of a purified leonardite humic acid modifies the transcriptional regulation of the main physiological root responses to Fe deficiency in Fe-sufficient cucumber plants. Plant Physiol Biochem 47:215–223

Álvarez-Fernández A, Garcıa-Marco S, Lucena JJ (2005) Evaluation of synthetic iron(III)-chelates (EDDHA/Fe^{3+}, EDDHMA/Fe^{3+} and the novel EDDHSA/Fe^{3+}) to correct iron chlorosis. Europ J Agronomy 22:119–130

Anderson CA (1983) The effect of FeEDDHA on the development of lime-chlorosis in two seedling populations of Eucalyptus obliqua L'Herit. Plant Soil 70:299–302

Antonopoulou C, Dimassi K, Therios I, Chatzissavvidis C, Papadakis I (2007) The effect of Fe-EDDHA and of ascorbic acid on in vitro rooting of the peach rootstock GF-677 explants. Acta Physiol Plant 29:559–561

Bar-ness E, Chen Y (1991) Manure and peat based iron-organo complexes. Plant Soil 130:35–43

Bell RW, Dell B (2008) Micronutrients for sustainable food, feed, fibre and bioenergy production. International Fertilizer Industry Association (IFA), Paris

Bitcover EH, Sieling DH (1951) Effect of various factors on the utilization of nitrogen and iron by Spirodela polyrhiza (l.) Schleid.1. Plant Physiol 26:290–303

Chassapis K, Roulia M, Nika G (2010) Fe(III)–humate complexes from Megalopolis peaty lignite: a novel eco-friendly fertilizer. Fuel 89:1480–1484

Chen Y, Clapp CE, Magen H (2004) Mechanisms of plant growth stimulation by humic substances: the role of organo-iron complexes. Soil Sci Plant Nutr 50(7):1089–1095

Chernyshov AA, Veligzhanin AA, Zubavichus YV (2009) Structural materials science end-station at the Kurchatov Synchrotron Radiation Source: recent instrumentation upgrades and experimental results. Nucl Instrum Meth A 603:95–98

Cornell RM, Schwertmann U (2003) The iron oxides, Structure, properties, reactions occurrences and uses. Wiley, Weinheim

Dickson DPE, Heller-Kallai L, Rozenson I (1980) Mossbauer spectroscopic studies of hufiic acid and fulvic acid soil fractions. J de physique Colloque C1(41):c1–409

Hansen EH, Mosbaek H (1970) Mossbauer studies of an iron(III)-fulvic acid complex. Acta Chem Scand 24:3083–3084

Herjsted LN (1991) Process for preparing preferred iron humates. 25.05.1993

Horneer CK, Burk D, Hoover SR (1934) Preparation of humate iron and other humate metals. Plant Physiol Biochem 9:663–669

Kovacs K, Kuzmann E, Fodor F, Vertes A, Kamnev AA (2005) Mössbauer study of iron uptake in cucumber root. Hyperfine Interact 165(1–4):289–294

Lakatos B, Korecz L, Meisel J (1977) Comparative study on the mossbauer parameters of iron humates and polyuronates. Geoderma 19:149–157

Levinskij BV (2002) Method for preparing complex humin fertilizers. Russian Federation Patent 2002

Lobartini JC, Tan KH, Pape C (1998) Dissolution of aluminum and iron phosphates by humic acids. Commun Soil Sci Plant Anal 29(5–6):535–544

Lovley DR, Woodward J, Blunt-Harris E, Hayes L, Phillips E, Coates J (1998) Humic substances as a mediator for microbially catalyzed metal reduction. Acta Hydrochim Hydrobiol 26:152–157

Mahesh K, Sharma ND, Gupta DC (1979) Mossbauer study of iron (III) salycilates. Proc Indian Natl Sci Acad, Part A 45:277–283

Mokronosov AT (1994) The small workshop on plant physiology. Moscow State University, Moscow

Morgan B, Lahav O (2007) The effect of pH on the kinetics of spontaneous Fe(II) oxidation by O_2 in aqueous solution—basic principles and a simple heuristic description. Chemosphere 68:2080–2084

Muscolo A, Sidari M, Attinà E, Francioso O, Tugnoli V, Tugnoli V (2007) Biological activity of humic substances is related to their chemical structure. Soil Sci Soc Am J 71:75–85

Nakamoto K (1986) Infrared and raman spectra of inorganic and coordination compounds. Wiley-Interscience, New York

Newville M (2001) IFEFFIT: interactive XAFS analysis and FEFF fitting. J Synchrotron Rad 8(2):322–324

Perez-Sanz A, Lucena JJ, Graham MC (2006) Characterization of Fe–humic complexes in an Fe-enriched biosolid by-product of water treatment. Chemosphere 65:2045–2053

Perminova I (2005) Humic acids metallic compound: preparation thereof, composition, preparation containing same and use of said compounds. Germany Patent 2005

Polyakov AY, Goldt AE, Sorkina TA, Perminova IV, Pankratov DA, Goodilin EA, Tretyakov YD (2012) Constrained growth of anisotropic magnetic δ-FeOOH nanoparticles in the presence of humic substances. CrystEngComm 14:8097–8102

Refait P, Gehin A, Abdelmoula M, Genin J-MR (2003) Coprecipitation thermodynamics of iron(II–III) hydroxysulphate green rust from Fe(II) and Fe(III) salts. Corros Sci 45:659–676

Ritchie JD, Perdue EM (2003) Proton-binding study of standard and reference fulvic acids, humic acids, and natural organic matter. Geochim Cosmochim Acta 67(1):85–96

Romheld V, Merschner H (1986) Evidence for a specific uptake system for iron phytosiderophores in roots of grasses. Plant Physiol 80(1):175–180

Schwertmann U, Cornell RM (2000) Iron oxides in the laboratory preparation and characterization. Wiley, Weinheim

Shenker M, Chen Y (2005) Increasing iron availability to crops: fertilizers, organo-fertilizers, and biological approaches. Soil Sci Plant Nutr 51(1):1–17

Stevenson FJ (1982) Humus chemistry: genesis, composition, reactions. Wiley, New York

Stevenson FJ, Goh KM (1971) Infrared spectra of humic acids and related substances. Geochim Cosmochim Acta 35:471–483

Walsh S, Lappin-Scott HM, Stockdale H, Herbert BN (1995) An assessment of the metabolic activity of starved and vegetative bacteria using two redox dyes. J Microbiol Methods 24:1–9

Yehuda Z, Hadar Y, Chen Y (2003) Immobilized EDDHA and DFOB as iron carriers to cucumber plants. J Plant Nutr 26(10&11):2043–2056